THE PRODUCTION OF J/Ψ IN 200 GeV/NUCLEON OXYGEN-URANIUM INTERACTIONS

NA38 Collaboration

C. BAGLIN, A. BUSSIERE, J.P. GUILLAUD, H. OGREN ¹, F. STALEY LAPP, CNRS-IN2P3, F-74019 Annecy-le-Vieux, France

A. BALDIT, J. CASTOR, A. DEVAUX, J. FARGEIX, X. FELGEYROLLES, P. FORCE, L. FREDJ, G. LANDAUD

LPC, Université de Clermont-Ferrand and CNRS-IN2P3, F-63001 Clermont-Ferrand Cedex, France

P. SONDEREGGER

CERN, CH-1211 Geneva 23, Switzerland

M.C. ABREU, G.P. BARREIRA, P. BORDALO, A. CASACA, A. FERRAZ, R. FERREIRA, J.M. GAGO, P. GOMES, C. LOURENÇO, A. MAIO, L. PERALTA, M. PIMENTA, S. RAMOS, J. VARELA

LIP, Lisbon, Portugal

C. GERSCHEL, A. SINQUIN

IPN, Université de Paris-Sud and CNRS-IN2P3, F-91405 Orsay Cedex, France

S. BORENSTEIN ², P. BUSSON, C. CHARLOT, B. CHAURAND, L. KLUBERG, A. ROMANA, R.A. SALMERON

LPNHE, Ecole Polytechnique and CNRS-IN2P3, F-91128 Palaiseau Cedex, France

J. BRITZ, P. GORODETZKY, L. KRAUS, I. LINCK, C. RACCA

CNR, CNRS-IN2P3 and Université Louis Pasteur, F-67037 Strasbourg Cedex, France

R. CASES

IFIC, Centro Mixto Universidad de Valencia-CSIC, E-46100 Burjasot, Valencia, Spain

M. ALIMI, M. BEDJIDIAN, D. CONTARDO, E. DESCROIX, O. DRAPIER, J.Y. GROSSIORD, A. GUICHARD, R. HAROUTUNIAN and J.R. PIZZI

IPN, Université de Lyon and CNRS-IN2P3, F-69622 Villeurbanne Cedex, France

Received 3 February 1989

¹ Visitor from Indiana University, Blooomington, IN 47405, USA.

² Present address: Cuny, York College, Jamaica, NY 11451, USA.

The study of oxygen-uranium reactions at 200 GeV/nucleon shows a significant transverse energy dependence of the yield of J/Ψ's relative to muon pairs produced in the mass continuum. This feature, observed for the first time, is in agreement with predictions from quark-gluon plasma formation, although alternative explanations by hadronic effects cannot be ruled out at this stage.

Non-perturbative OCD predicts that extreme conditions of temperature and/or density induce a phase transition in hadronic systems, leading to the deconfinement of quarks and gluons of ordinary matter and to the formation of a quark-gluon plasma (QGP) [1]. According to these predictions, the conditions required for the phase transition could be reached in ultrarelativistic heavy ion collisions. Among several signatures which have been proposed in order to identify the QGP formation, the suppression of the J/Ψ production has been pointed out by Matsui and Satz [2]. They assume that the binding potential necessary for the cc pair to form a J/Y is screened inside the plasma above a certain temperature, so that the bound state can only appear if formed outside the hot volume [2, 3].

The first experimental study of these predictions became possible with the availability of intense ion beams of 200 GeV/nucleon, successfully delivered, for the first time in the fall of 1986, by the CERN accelerators. The goal of the NA38 experiment at CERN is to measure the production of muon pairs originating from virtual photons and vector mesons, in correlation with the energy density of the collision, estimated from the transverse energy deposited in an electromagnetic calorimeter. This paper reports results on the J/ Ψ production in 200 GeV/nucleon ox-

ygen-uranium interactions. Preliminary results obtained while the analysis was still in progress can be found elsewhere [4].

The detector [5] consists mainly of a muon spectrometer and an electromagnetic calorimeter. The low probability to produce a muon pair in a hadronic interaction requires a high luminosity, achieved with an intense incident beam (of the order of several 10⁷ ions/burst) and a 20% interaction length target. Under such extreme conditions, beam counters and a segmented active target are needed to reject pile-up and events with a reinteracting spectator fragment which can lead to an incorrect measurement of the transverse energy of the reaction.

The muon spectrometer, already used in the CERN NA10 experiment [6], is shown in fig. 1. It is separated from the target region by a 4.8 m long hadron absorber made of carbon with a tungsten-uranium central plug to absorb the beam particles which do not interact in the target. The air-core magnet, with hexagonal symmetry, produces a toroidal field which leads to a bending angle inversely proportional to the transverse momentum of the muon. With a current of 4000 Λ , the field is B_{φ} =0.29 T at a mean radius r=75 cm and $\int B \, dl$ =1.2 Tm. Four plastic scintillator hodoscopes, R1-R4, provide the trigger. A muon is defined by the quadruple coincidence of two counters

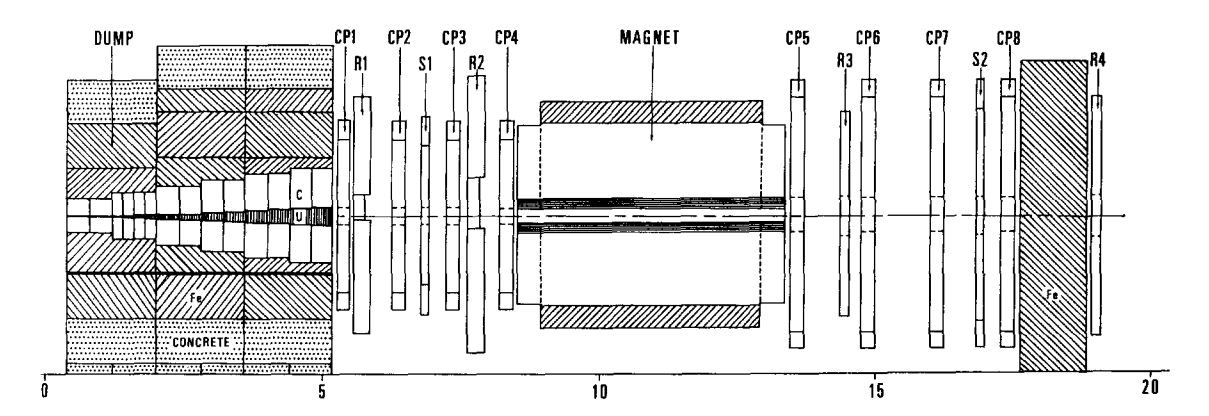


Fig. 1. Lay-out of the muon spectrometer.

of R1 and R2 which select particles pointing to the target, and two counters R3 and R4 which allow a fast estimate of its transverse momentum. The trigger requires two such coincidences in different sextants. Two sets of four multiwire proportional chambers, CP1-CP4 and CP5-CP8, located respectively upstream and downstream of the magnet, measure the muon tracks. The spectrometer detects dimuons in the rapidity 2.8 < y < 4 in the laboratory. Mass resolution is essentially due to multiple scattering for masses lower than $3 \text{ GeV}/c^2$ and is about $0.15 \text{ GeV}/c^2$. Acceptances in mass M, rapidity and transverse momentum P_T of the muon pairs are of the order of 10%.

A schematic lay-out of the detectors associated with the spectrometer is shown in fig. 2. The multiple target [7] consists of ten rectangular uranium subtargets, 1 mm thick each, with transverse dimensions of $10 \times 10 \text{ mm}^2$ for the first one and $3 \times 1 \text{ mm}^2$ for the others, adapted to an actual beam spot size of $\sigma = 0.5$ mm. The subtargets are separated by 24 mm intervals and are surrounded by 24 ring scintillators. The pulse height pattern of the scintillators allows to identify the location of the primary interaction and of reinteracting spectators, if any. The large spacing between the subtargets and their small area are needed to minimize reinteractions of photons and improve, consequently, the performance of this identification.

The electromagnetic calorimeter [8] is made of 1 mm diameter scintillating fibers embedded in lead in a 1:2 volume ratio. The 12 cm long (15 radiation

lengths) converter has an outer radius of 12 cm and an inner radius of 1.2 cm. Its front face is located 32 cm downstream of the target center. It covers the pseudo-rapidity range $1.7 < \eta < 4.1$. The readout is divided into sextants, according to the general geometry of the apparatus, and each sextant is divided into five sectors corresponding to roughly equal pseudo-rapidity bins. The transverse energy for an element i is $E_{Ti}^0 \sin \theta_i$, where θ_i is calculated off-line using the position of the primary interaction. Such a calorimeter would have a poor resolution if we had to measure the energy of a single particle, because the dimensions of its smallest elements are comparable with the size of an electromagnetic shower. In fact, we measure an energy flow and, in that case, the resolution increases with the multiplicity. A Monte Carlo calculation based on GEANT.3 leads to a resolution $\sigma(E_{\rm T})/E_{\rm T}$ of 5% for oxygen-uranium central collisions. It also shows that the contamination of charged particles results in a measured transverse energy which is 1.5 times higher than the neutral transverse energy, assuming a ratio of 2 between charged and neutral particles.

A beam hodoscope [9] is used to count and identify each ion, as well as to reject events where another ion contaminates the signals of the calorimeter and active target measured within the 20 ns wide gate of the ADC's. It is made of two parallel planes of 14 and 16 plastic scintillators respectively, 1 mm thick each. It is located 33 m upstream of the target, in a region where the beam spot is wide enough to reduce indi-

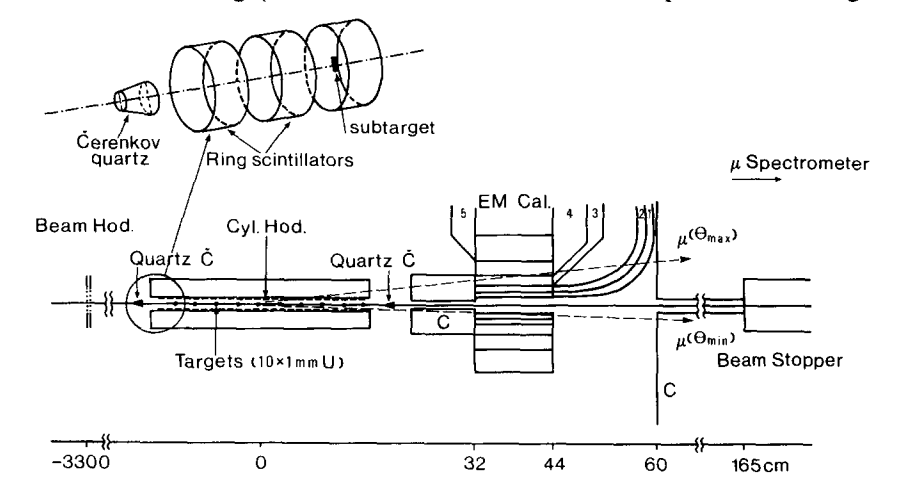


Fig. 2. Lay-out of the electromagnetic calorimeter, the active target and the beam detectors.

vidual counting rates and avoid radiation damage. Further redundancy is provided by two 3 mm thick quartz Čerenkov counters [10], insensitive to the high level radiation, located at both ends of the active target. They are divided into four quadrants, which allows to center the beam on the subtargets with a 50 μ m accuracy. The interaction rate is finally monitored by three scintillator telescopes pointing at 90° to the target.

The average intensity of the incident beam was 3×10^7 ions per burst, with a spill of 2.8 s, leading to 6×10^6 interactions/burst. The first level trigger required two muons and fired at a rate of 600 events per burst. A second level trigger, based on the rejection of events where both muons had a transverse momentum lower than $0.26 \, \text{GeV}/c$, led to about 250 events per burst, with an acquisition live-time greater than 90%. A total amount of 4.5×10^6 events were finally written on tape.

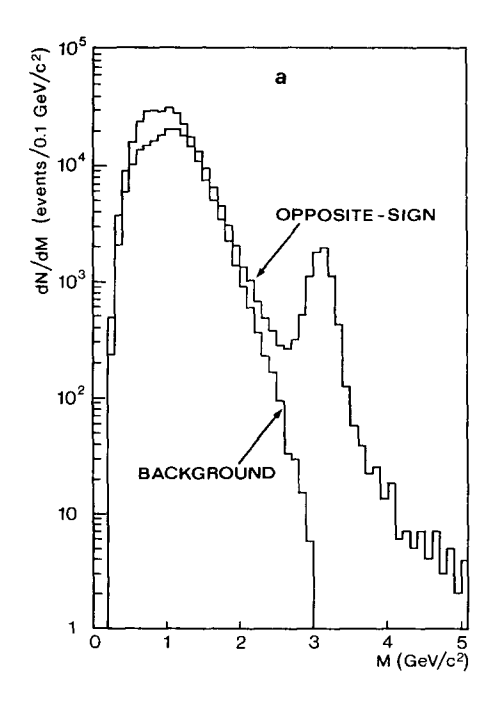
The offline treatment requires that at least two tracks in the air sectors of the magnet are reconstructed from the hits in the proportional chambers and that the corresponding trigger counters are fired; the tracks must be in two different sextants and have a common origin in the target region. These first re-

quirements lead to a sample of 1.7×10^6 reconstructed events. A further selection is made according to the following criteria:

- The active target algorithm identifies one interaction and only one. This condition rejects events where two ions have interacted in two different subtargets and events where the projectile spectator reinteracts in a subsequent subtarget.
- One and only one incident ion is detected by the beam hodoscope and the quartz counters within the 20 ns gate opened by the trigger. This beam condition selects events totally free from pile-up at the price, however, of rejecting also events where the second incident ion has not interacted.
- Two and only two tracks satisfy the reconstruction requirements. The corresponding rejection of events with more than two muons is less than 1%.

The kinematical parameters of the muons are then computed by assigning their origin at the center of the identified subtarget. After this selection, the remaining number of events amounts to 8.5×10^5 .

In the following analysis, we study the yield of J/Ψ 's as a function of the energy density estimated from the measured transverse energy E_T . In order to compare this yield in different E_T bins, we need to



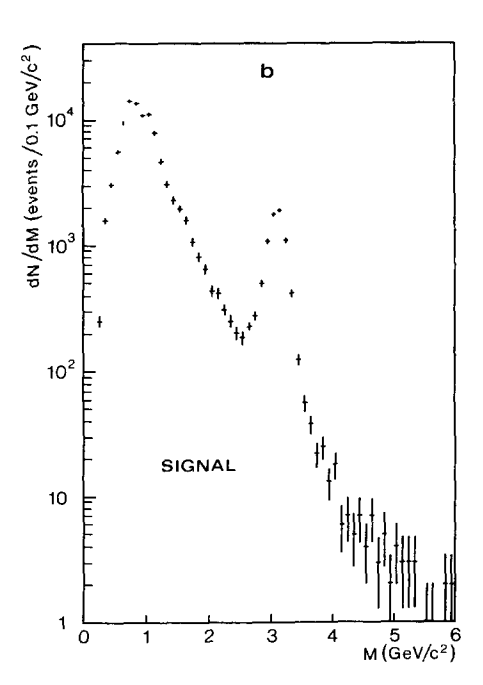


Fig. 3. The mass spectra for opposite-sign and background muon pairs (a) and for the signal (b).

normalize the number of produced J/Y's to some process of understood physical meaning, for instance to muon pairs produced by the Drell-Yan mechanism. Both the J/Ψ's and Drell-Yan events lead to opposite-sign muon pair events. Opposite-sign pairs originate also from the production and decay into muons of low-mass vector mesons, DD pairs, and Ψ' 's; the main contribution to this sample, however, is due to multiple π and K meson production and decay, called from hereon the "background". The π and K decays lead also to like-sign pairs which are used to estimate this background in the sample of opposite-sign dimuons. We assume that the probability to detect a muon of any sign in our apparatus is independent of the sign of the second one and that the muon multiplicity distribution obeys a Poisson law. The number of background events is then given by $2\sqrt{N^{++}N^{--}}$, where N^{++} and N^{--} are the numbers of $\mu^+\mu^+$ and $\mu^-\mu^-$, respectively. The signal is then obtained by subtracting differentially in mass and $P_{\rm T}$, for different intervals of $E_{\rm T}$, this background from the total number of opposite-sign muon pairs, N^{++} , according to the formula

Signal⁺⁻=
$$N^{+-}-2\sqrt{N^{++}N^{--}}$$
. (1)

Because of the limited statistics of our sample of events, this procedure systematically underestimates the background. The resulting bias does not exceed 20% and is independent of the transverse energy $E_{\rm T}$.

Fig. 3 shows the mass spectra of opposite-sign background and signal muon pairs, not corrected for acceptance, as is the case for all distributions presented in this letter. The signal to background ratio is 0.5 for a mass of $2 \text{ GeV}/c^2$ and is larger than 100 at the J/Ψ peak. In order to keep a good statistics to estimate the continuum and, at the same time, minimize the effects of the decays of charmed mesons, we perform the analysis only for dimuons of mass greater than 1.7 GeV/ c^2 . This final sample contains about 12 000 events and more than half of them are J/Ψ 's.

The numbers of J/Ψ 's and of muon pairs in the continuum are obtained from the data according to the following procedure. The mass spectrum is fitted to an expression which represents a superposition of a continuum, given by an exponential divided by M^3 and two gaussians for the J/Ψ and the Ψ' , respectively:

$$dN/dM = N_0 \exp(-M/M_c)/M^3 + N_1 \exp[-(M-M_{\Psi})^2/2\sigma_{\Psi}^2] + N_2 \exp[-(M-M_{\Psi'})^2/2\sigma_{\Psi'}^2].$$
 (2)

The fit is done using the maximum likelihood method. The free parameters are M_c , related to the shape of the continuum, and the constant N_0 , N_1 and N_2 , constrained by the absolute normalization. M_{Ψ} , $M_{\Psi'}$, σ_{Ψ} and $\sigma_{\Psi'}$ are the standard masses and the experimental resolutions of the J/ Ψ and Ψ' respectively, which are fixed inputs to the fit. In a separate check of the reconstruction procedure we obtain the fitted values $M_{\Psi} = (3.102 \pm 0.003) \text{ GeV}/c^2$, very close to the value given by the Particle Data Group tables [11], and $\sigma_{\Psi} = (0.145 \pm 0.003) \text{ GeV}/c^2$, in agreement with the mass resolution of the spectrometer.

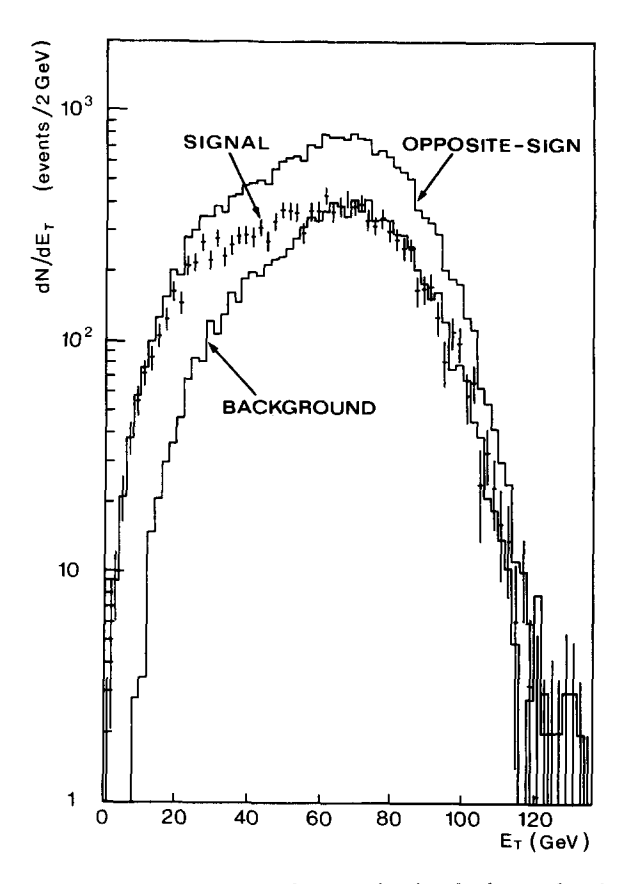


Fig. 4. The E_T -distribution for opposite-sign, background and signal muon pairs.

From the fitted values of the parameters, we compute analytically the number N_{Ψ} of J/ Ψ 's and the number N_c of continuum events in the J/ Ψ mass region $(2.7 < M < 3.5 \text{ GeV}/c^2)$ and define the ratio $S = N_{\Psi}/N_c$. The dependence of the J/ Ψ production on the transverse energy is studied by calculating the ratio S in six E_T intervals. These intervals contain ap-

proximately equal numbers of signal events and correspond hence to unequal shares of the differential minimum biased cross section, of which the first $E_{\rm T}$ bin covers roughly 74% and the last one 3%. Fig. 4 shows the distributions of the measured transverse energy $E_{\rm T}$, associated with opposite-sign, background and signal muon pairs, with masses higher

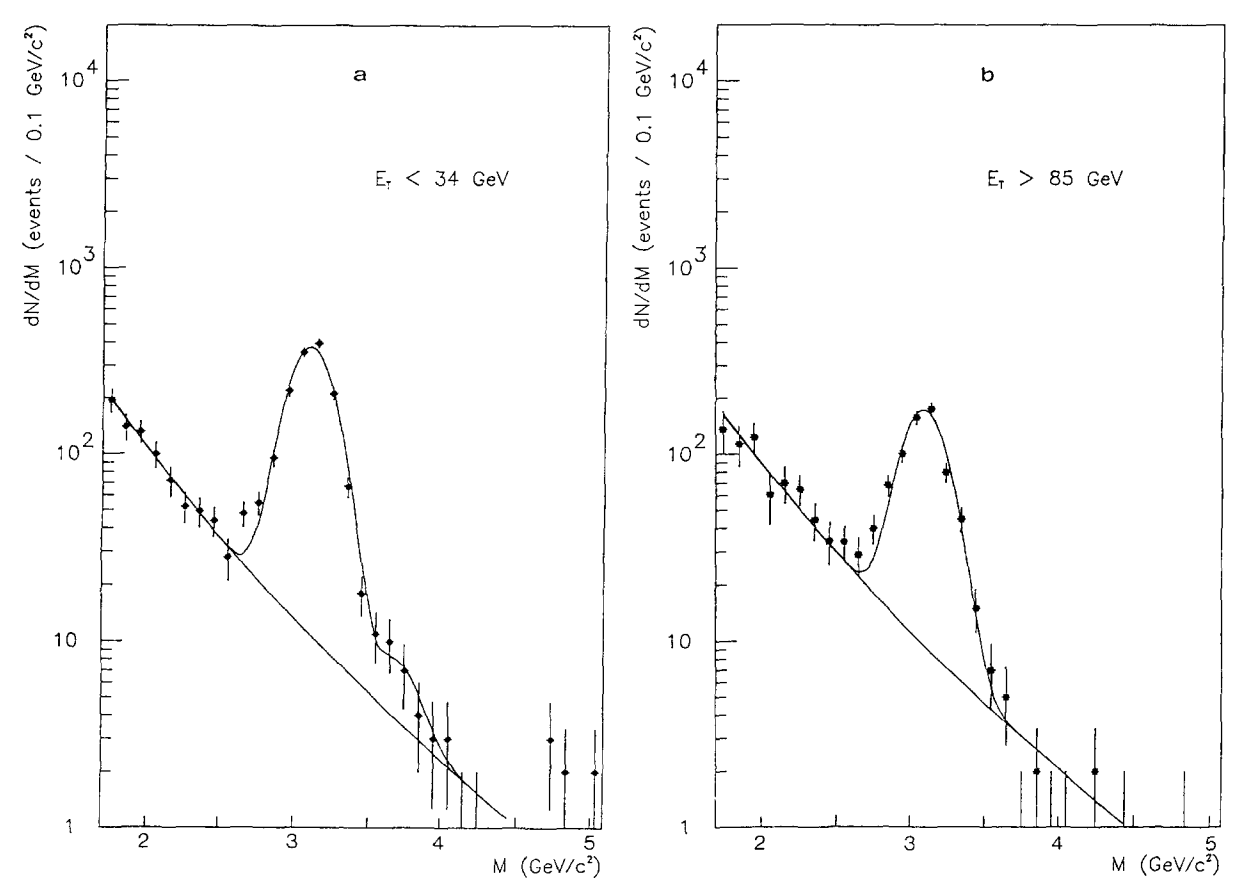


Fig. 5. Mass spectrum and fit of the signal muon pairs in two different E_T bins: $E_T < 34$ GeV (a) and $E_T > 85$ GeV (b).

Table 1 Values of S, M_c and R for the six E_T intervals. Only statistical errors are quoted.

$E_{T}(GeV)$	$M_{\rm c}({\rm GeV}/c^2)$	S	R	χ^2/dof
$E_{\rm T}$ < 34	1.14±0.14	13.8 ± 1.7	1	0.8
$34 < E_T < 49$	1.35 ± 0.19	12.3 ± 1.4	0.89 ± 0.15	1.0
$49 < E_{\rm T} < 62$	1.21 ± 0.12	11.2 ± 1.0	0.81 ± 0.12	0.7
$62 < E_{\rm T} < 72$	1.04 ± 0.12	11.2 ± 1.5	0.81 ± 0.14	0.9
$72 < E_{\rm T} < 85$	1.28 ± 0.15	9.0 ± 2.0	0.65 ± 0.11	0.6
$E_{\rm T} > 85$	1.19 ± 0.14	7.2 ± 0.9	0.52 ± 0.09	0.6
all $E_{ m T}$	1.13 ± 0.06	13.3 ± 0.7	_	1.5

than 1.7 $\,\mathrm{GeV}/c^2$. The fall of the spectrum in the low E_T region, which corresponds to peripheral collisions, is due to the muon pair trigger and to the requirement of subtarget identification, which both favour central collisions. Figs. 5a and 5b show the fitted mass spectra in the two extreme intervals, $E_\mathrm{T} < 34$ GeV and $E_\mathrm{T} > 85$ GeV.

Table 1 gives the values of S and M_c for the six E_T intervals, as well as the ratios R of the different values of S relative to the one obtained in the lowest E_T interval ($E_T < 34 \text{ GeV}$). Fig. 6 displays the evolution of S with E_T . The values of S show a clear decrease of the J/ Ψ production relative to the continuum with increasing transverse energy. The value of R for $E_T > 85 \text{ GeV}$ is $R = 0.52 \pm 0.09$. The values of S will obviously change after acceptance correction. However, a preliminary study indicates that this acceptance correction does not affect significantly the evolution of S and R with E_T . It should be pointed out that results are unchanged if the lower limit of the fitted mass interval is moved from 1.7 to 2.1 GeV/ c^2 , whereas the signal to background ratio increases

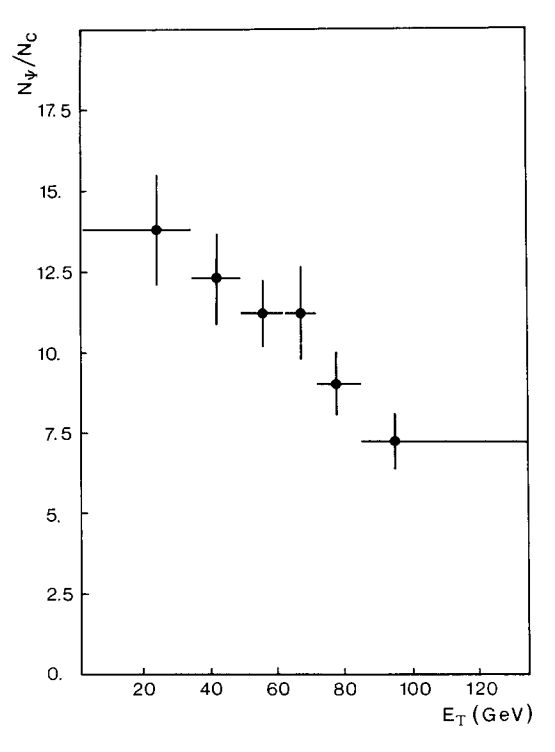


Fig. 6. The evolution of $S = N_{\Psi}/N_c$ as a function of E_T .

by a factor of two. Furthermore, a significant residual contamination of background events would change the shape of the continuum spectrum in the different $E_{\rm T}$ bins, in contradiction with the observed stability of $M_{\rm c}$. It is therefore unlikely that the observed $E_{\rm T}$ dependence is due to an inadequate background subtraction procedure.

The J/Ψ suppression has been predicted as an unambiguous signature of the quark–gluon plasma formation [2]. Several calculations have also been made recently to explain our results. They are based either on final state interactions [12] or on distortions of the initial state in a nuclear environment [13]. These different interpretations will have to be compared with experimental data obtained with other projectiles and targets in a study including other variables, in particular the transverse momentum of the muon pair.

In conclusion, the study of J/ Ψ production in 200 GeV/nucleon oxygen-uranium interactions shows that the ratio S of the number of J/ Ψ 's over the number of muon pairs in the mass continuum between 2.7 and 3.5 GeV/ c^2 decreases with increasing transverse energy, i.e. with increasing energy density. In particular, S changes by a factor 0.52 ± 0.09 between our two extreme E_T intervals. Although the J/ Ψ suppression has been predicted as a signature of QGP formation, it is not excluded that alternative mechanisms could explain, at least partly, our experimental results.

We wish to thank all the experts of CERN, GSI and LBL who have made possible the development and acceleration of ion beams at CERN. We also thank the EA group and particularly H. Atherton for their work on our beam line. We are grateful to the technical staff of the Collaboration for their work on the detector design, construction and setting-up.

References

K. Kajantie, ed., Quark Matter '84, Proc. 4th Intern. Conf. on Ultrarelativistic nucleus-nucleus collisions, Lecture Notes in Physics, Vol. 221 (Springer, Berlin, 1984).
 L.S. Schroeder and M. Gyulassy, eds., Quark Matter '86, Proc. 5th Intern. Conf. on Ultrarelativistic nucleus-nucleus collisions, Nucl. Phys. A 467 (1987) 1;

- R. Stock, H. Specht and H. Satz, eds., Quark Matter '87, Proc. 6th Intern. Conf. on Ultrarelativistic nucleus-nucleus collisions, Z. Phys. C (1988), to be published;
- S. Raha and B. Sinha, eds., Proc. Intern. Conf. on Physics and astrophysics of quark-gluon plasma (Bombay, 1988) (World Scientific, Singapore, 1988) to be published.
- J.D. Bjorken, Phys. Rev. D 27 (1983) 140.
- [2] T. Matsui and H. Satz, Phys. Lett. B 178 (1986) 416.
- [3] F. Karsch, M.T. Mehr and H. Satz, Z. Phys. C 37 (1988) 617.
- [4] C. Gerschel (NA38 Collab.), in: Hadrons, quarks and gluons, ed. J. Tran Thanh Van (Editions Frontières, Gifsur-Yvette, France, 1987) p. 443;
 - A. Romana (NA38 Collab.), in: Proc. Intern. Europhysics Conf. on High energy physics (Uppsala) ed. O. Bodner (Uppsala, 1987) p. 150; in: Proc. Intern. Conf. on Physics and astrophysics of quark-gluon plasma (Bombay, 1988) (World Scientific, Singapore, 1988), to be published;
 - A. Bussière (NA38 Collab.), in: Proc. Quark Matter '87, Z. Phys. C (1988) 117;
 - S. Ramos (NA38 Collab.), Proc. IXth Automn Lisbon School (World Scientific, Singapore, 1988), to be published. P. Bordalo (NA38 Collab.), in: Proc. Rencontres the Moriond (Editions Frontières, Gif-sur-Yvette, 1988), to be published;
 - L. Kluberg (NA38 Collab.), in: Proc. IXth Intern. Seminar on High energy physics problems, relativistic nuclear physics and quantum chromodynamics (Dubna, June 1988), to be published;

- P. Sonderegger (NA38 Collab.), in: Proc. XXIVth Intern. Conf. on High energy physics (Munich, August 1988), to be published;
- J.Y. Grossiord (NA38 Collab.), in: Proc. of Quark matter '88 (Lenox, September 1988), to be published;
- C. Racca (NA38 Collab.), in: Proc. Hadronic matter in collision (Tucson, October 1988), to be published;
- D. Contardo (NA38 Collab.), in: II Entretiens Jacques Cartier (Montréal, October 1988), to be published.
- [5] M. Abreu et al., Nucl. Instrum. Methods, to be published.
- [6] L. Anderson et al., Nucl. Instrum. Methods 223 (1984) 26.
- [7] M. Alimi, Thesis, Université Claude Bernard, Villeurbanne (1988), unpublished.
- [8] A. Devaux (NA38 Collab.), in: Proc. Quark Matter '88 (Lenox, September 1988) to be published.
- [9] A. Sinquin, Thesis, Université Paris XI, Orsay (1988), unpublished.
- [10] C. Charlot, Thesis, Université Louis Pasteur, Strasbourg (1988), unpublished.
- [11] Particle Data Group, G.P. Yost et al., Review of Particle Properties, Phys. Lett. B 204 (1988) 32.
- [12] C. Gerschel and J. Huefner, Phys. Lett. B 207 (1988) 259;A. Capella et al., Phys. Lett. B 206 (1988) 354;
 - J. Ftacnik et al., Phys. Lett. B 207 (1988) 194;
 - J.P. Blaizot and J.Y. Ollitrault, Preprint Saclay SPhT/88-
 - 111; and Phys. Rev. D, to be published;
 - S. Gavin et al., Phys. Lett. B 207 (1988) 257.
- [13] A.V. Efremov et al., preprint JINR Dubna (1988).